

New isotopic evidence bearing on bonanza (Au-Ag) epithermal ore-forming processes

James A. Saunders¹ · Ryan Mathur² · George D. Kamenov³ · Toru Shimizu⁴ · Matthew E. Brueseke⁵

Received: 8 July 2015 / Accepted: 4 November 2015 / Published online: 18 November 2015
© Springer-Verlag Berlin Heidelberg 2015

Abstract New Cu, S, and Pb isotope data provide evidence for a magmatic source of metal(loid)s and sulfur in epithermal Au-Ag deposits even though their ore-forming solutions are composed primarily of heated meteoric (ground) waters. The apparent isotopic discrepancy between ore metals and ore-forming solutions, and even between the ore and associated gangue minerals, indicates two different sources of epithermal ore-forming constituents: (1) a shallow geothermal system that not only provides the bulk of water for the ore-forming solutions but also major chemical constituents leached from host rocks (silica, aluminum, potassium, sodium, calcium) to make gangue minerals and (2) metals and metalloids (As, Te, Sb, etc.) and sulfur (\pm Se) derived from deeper magma bodies. Isotopic data are consistent with either vapor-phase transport of metal(loid)s and sulfur and their subsequent absorption by shallow geothermal waters or formation of metallic (Au, Ag, Cu phases) nanoparticles at depth from magmatic fluids prior to encountering the geothermal system. The latter is most

consistent with ore textures that indicate physical transport and aggregation of nanoparticles were significant ore-forming processes. The recognition that epithermal Au-Ag ores form in tectonic settings that produce magmas capable of releasing metal-rich fluids necessary to form these deposits can refine exploration strategies that previously often have focused on locating fossil geothermal systems.

Keywords Epithermal ores · Copper isotopes · Sulfur isotopes · Lead isotopes · Magmatic source · Nanoparticles

Introduction

Epithermal ores have accounted for a significant proportion of historic Au and Ag production worldwide (7 and 16 %, respectively; Simmons et al. 2005). Epithermal deposits are formed under relatively shallow, low-temperature conditions and occur worldwide in subduction-related volcanic arcs, back-arc rift zones, and postsubduction volcanic settings (Simmons et al. 2005; Richards 2009; Saunders and Brueseke 2012). Their ore-forming solutions appear to be largely heated meteoric (ground) water similar to present-day geothermal systems based on H and O isotope studies (O’Neil et al. 1973; John et al. 2003; Simmons et al. 2005; Saunders et al. 2008), although some studies suggest that there could be a significant component of magmatic waters involved in the main epithermal Au-Ag ore-forming stage (Matsuhisa and Aoki 1994; Hayashi et al. 2000; Faure et al. 2002). The source(s) of ore-forming constituents in these shallow ores is controversial, with some models proposing that metals and sulfur are leached from surrounding country rocks, in contrast to others invoking a magmatic source for metals and sulfur, with perhaps some degree of mixing of the two potential sources. More recently, Heinrich et al. (2004)

Editorial handling: B. Lehmann

✉ James A. Saunders
saundja@auburn.edu

¹ Department of Geosciences, 210 Petrie Hall, Auburn University, Auburn, AL 36849, USA

² Department of Geology, Juniata College, 1700 Moore Street, Huntingdon, PA 16652, USA

³ Department of Geological Sciences, University of Florida, 241 Williamson Hall, P.O. Box 112120, Gainesville, FL 32611, USA

⁴ Magma-hydrothermal deposits Research Group, Geological Survey of Japan, AIST, 1-1-1 Higashi, Tsukuba 305-8567, Japan

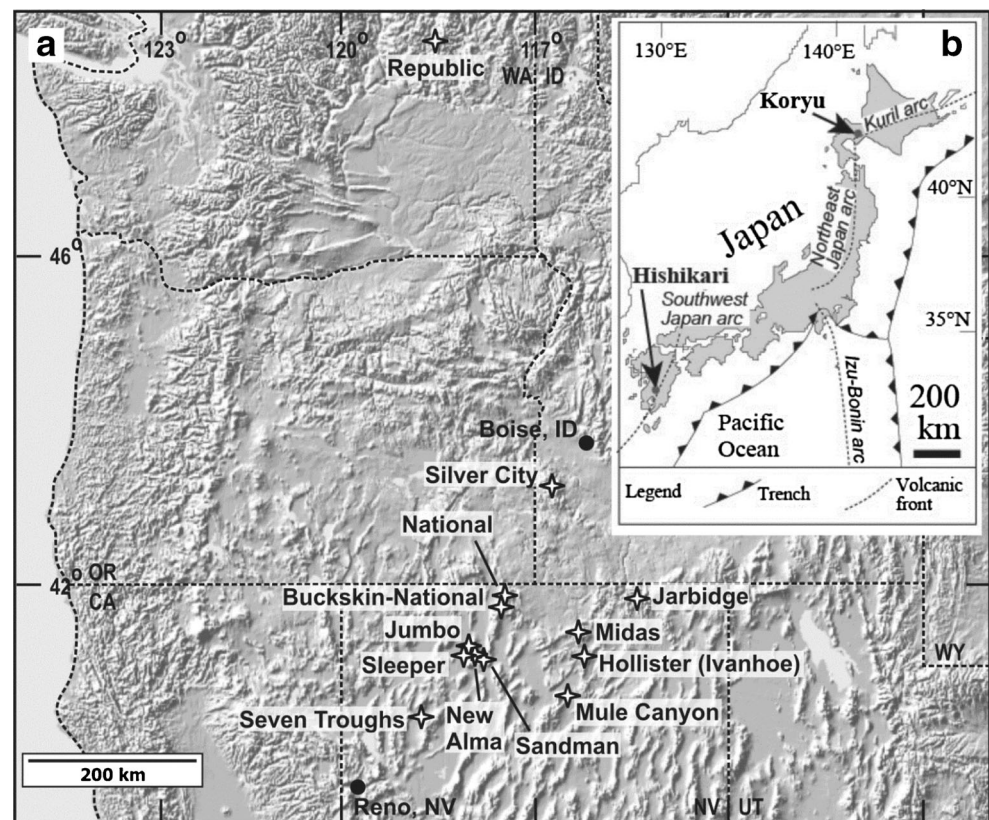
⁵ Department of Geology, Kansas State University, Manhattan, KS 66506, USA

and Williams-Jones and Heinrich (2005) have proposed that low-density magmatic fluids can transport significant amounts of ore metals and sulfur from the deeper magmatic setting to the shallow epithermal systems. This so called vapor-phase transport of metals can be seen in present-day volcanic fumaroles, where micrometer to sub-micrometer-sized native gold particles (locally alloyed with Ag, Cu) and other metallic phases precipitate directly from volcanic emissions (Meeker et al. 1991; Fulignati and Sbrana 1998; Taran et al. 2000; Yudovskaya et al. 2006). Detailed textural studies of bonanza epithermal ores have shown, at least locally, that nanoparticles (or colloids) of Au-Ag-Cu minerals can be physically transported by epithermal ore-forming solutions, and their aggregation and deposition can form spectacularly high-grade ores (Saunders 1990, 1994, 2012; Marinova et al. 2014). Saunders and Schoenly (1995) and Marinova et al. (2014) proposed that boiling of the epithermal ore-forming solutions led to nanoparticle formation at shallow crustal settings. However, Pb and Re-Os isotope data from these bonanza ores support a deep, magmatic source of metals in these shallow ores (Kamenov et al. 2007; Saunders et al. 2008, 2014). Thus, this study was designed primarily to evaluate Cu and S isotopic constraints on the origin of ore-forming constituents in these ores, as well as to look at Pb isotope values in both ore and gangue minerals from the high-grade vein bands.

Results from these previous studies suggest that Au and Ag appear to be derived from mafic magmatic sources and not the adjacent host rocks. Further, the surrounding host rocks vary greatly in composition and age, yet the epithermal ores are remarkably similar in many respects (Saunders et al. 2008). Here, we present Cu isotope data from epithermal ores from western USA and Japan, along with well-constrained new Pb and S isotope data. All of these data strongly support a magmatic source of both metals and sulfur in epithermal ores and are also consistent with, but do not conclusively prove, nanoparticle transport of metals and sulfur. In addition, the new Pb isotope data support a different source for ore and gangue minerals in some epithermal ores.

There have been many attempts to classify these epithermal ores; Lindgren (1933) proposed a ninefold classification of them based mostly on mineralogy and geochemistry. However, today, two principal end-member types are currently recognized (Sillitoe and Hedenquist 2003; Simmons et al. 2005): (1) The most abundant class by far is generally referred to as “low sulfidation” (LS), deposited from near-neutral pH hydrothermal solutions and (2) “high-sulfidation”, deposits formed from acidic ore solutions. Here, we focus on some examples of the more abundant LS ores from two of the best-documented regions, western USA and Japan (Fig. 1). LS bonanza ores from both countries are renowned for their extraordinarily rich Au-Ag grades, and because of the

Fig. 1 Location map showing deposits or districts in the western USA and Japan where we recognize colloid aggregation textures. A subset of these deposits is discussed in the text



abundance of precious-metal minerals, it is possible to discern ore depositional features such as timing and mutual association of ore and gangue minerals, which allowed for an optimization of isotopic analyses. The northern Great Basin (USA) (NGB) mid-Miocene bonanza ores are thought to be related to the volcanism attending the initial emergence of the Yellowstone mantle plume (Saunders et al. 2008), whereas the Japanese ores are associated with volcanism in a subduction-back-arc rifting setting (Izawa et al. 1990; Shimizu et al. 1998).

Bonanza ores in both regions are characterized by banded, open space-filling vein textures, with electrum as the principal Au phase, whereas Ag is hosted by sulfides, sulfosalts, and selenides, although naumannite (Ag_2Se) and aguilarite (Ag_4SeS) are often the most abundant phases (Shimizu et al. 1998; Saunders et al. 2008). Quartz, opal, chalcedony, calcite, quartz-replacing calcite, and adularia are the common associated vein minerals, and chalcocopyrite is the most abundant base-metal sulfide mineral associated with Au-Ag minerals

(Fig. 2a). A hallmark of these ores is their banded nature, reflecting multiple Au-Ag depositing events (Fig. 2b). Highest-grade bands contain fractal dendrites of electrum-opal (Fig. 2c, d), naumannite-aguilarite, and locally, chalcocopyrite, which have been interpreted to have formed by aggregation of metallic nanoparticles (Saunders 1990, 1994, 2012). Although the deposits considered here are ≤ 16 Ma, such gold nanoparticle aggregation textures in epithermal ores have also been recognized in Cambrian deposits (Foley and Ayuso 2012).

Materials and methods

Data presented here are from petrographically well-characterized ore and gangue minerals from bonanza gold-silver ores, including the Sleeper, Midas, National, Buckskin National deposits (Nevada), Silver City district (Idaho), and the Koryu and Hishikari deposits (Japan) (Tables 1 and 2).

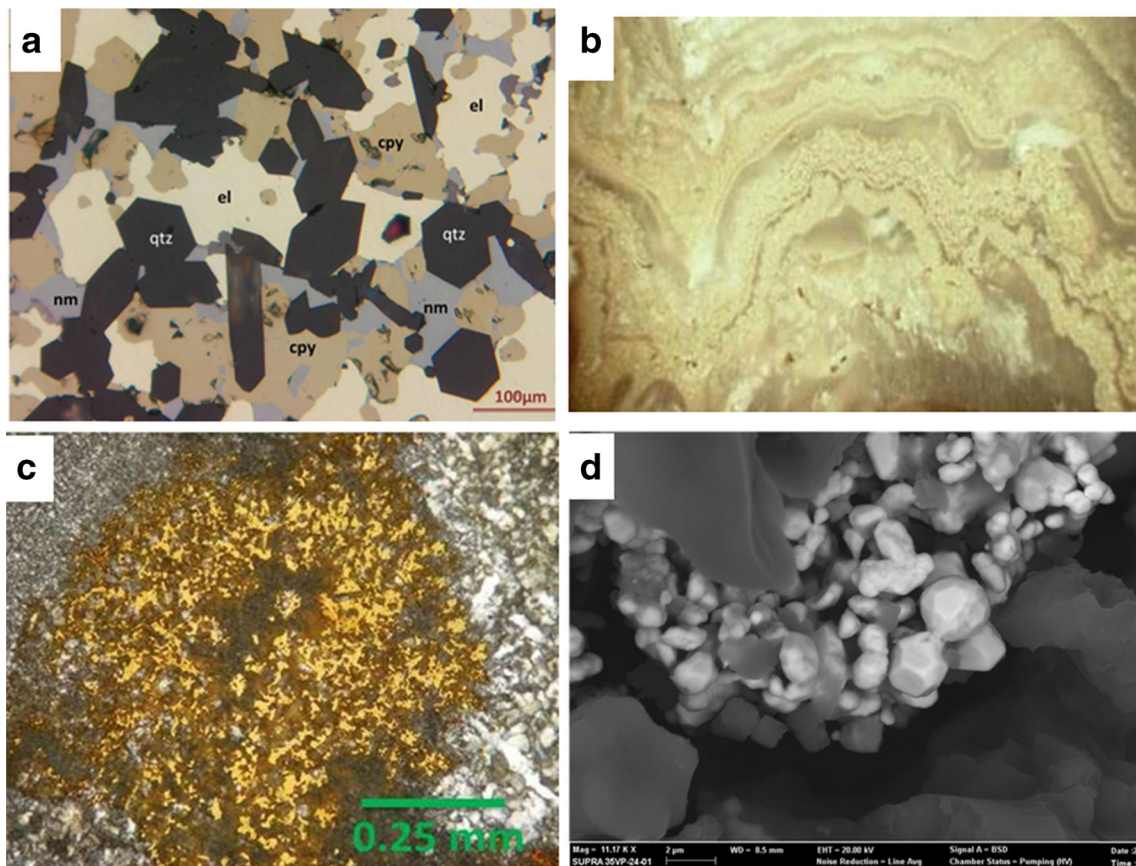


Fig. 2 **a** Photomicrograph (reflected light) showing typical rich Au-Ag “ginguro” ore from the Hishikari deposit, Kyushu, Japan. Mineral abbreviations: *el* electrum, *cpy* chalcocopyrite, *nm* naumannite, *qtz* quartz. **b** Photograph of multiple electrum and opal bands from the Sleeper deposit, Nevada (field of view is 7 cm). **c** Photomicrograph (transmitted and reflected light) of a fractal electrum dendrite in opal and quartz (*gray*)

from the Sleeper deposit (from Saunders 2012). **d** SEM image of a fractal dendrite similar to the one shown in (c) of electrum exposed by dissolving host silica with HF. This texture is interpreted to form by aggregation of physically transported electrum nanoparticles and crystals (Saunders 1994, 2012)

Table 1 Pb isotope data for electrum and gangue from the northern Nevada epithermal deposits

	$^{206}\text{Pb}/^{204}\text{Pb}$	$^{207}\text{Pb}/^{204}\text{Pb}$	$^{208}\text{Pb}/^{204}\text{Pb}$	Data source
^a Sleeper electrum	18.919	15.624	38.631	this work
S4a electrum	18.903	15.625	38.648	this work
S5 electrum	18.921	15.622	38.628	this work
S5a electrum	18.915	15.618	38.612	this work
S5b electrum	18.923	15.62	38.621	this work
S6 electrum	18.913	15.619	38.616	this work
S7 electrum	18.915	15.621	38.626	this work
S8 electrum	18.928	15.624	38.633	this work
S1 gangue	18.925	15.633	38.664	this work
S2 gangue	18.973	15.635	38.664	this work
S3 gangue	18.913	15.631	38.662	this work
S4 gangue	18.918	15.631	38.656	this work
S5 gangue	18.932	15.634	38.662	this work
S6 gangue	18.916	15.629	38.648	this work
S7 gangue	18.92	15.631	38.654	this work
S8 gangue	18.931	15.632	38.661	this work
S9 gangue	18.942	15.637	38.676	this work
National electrum	18.877	15.619	38.731	Kamenov et al. (2007)
Jumbo electrum	18.83	15.629	38.811	Kamenov et al. (2007)
Seven Troughs electrum	18.887	15.618	38.589	Kamenov et al. (2007)
Sleeper electrum	18.909	15.627	38.652	Kamenov et al. (2007)
Sleeper electrum	18.905	15.625	38.652	Kamenov et al. (2007)
Sleeper electrum	18.902	15.621	38.639	Kamenov et al. (2007)
National gangue	18.883	15.645	38.802	Kamenov et al. (2007)
National gangue	18.892	15.638	38.796	Kamenov et al. (2007)
National gangue	18.897	15.641	38.803	Kamenov et al. (2007)
Jumbo gangue	18.817	15.645	38.789	Kamenov et al. (2007)
New Alma gangue	19.001	15.661	38.89	Kamenov et al. (2007)
Sandman gangue	19.163	15.644	38.829	Kamenov et al. (2007)
Ivanhoe gangue	19.995	15.717	39.39	Kamenov et al. (2007)
Midas gangue	19.448	15.687	39.094	Kamenov et al. (2007)
Orofino Silver City gangue	19.058	15.664	39.018	Kamenov et al. (2007)
Sleeper gangue	18.904	15.622	38.637	Kamenov et al. (2007)

^aNumber corresponding to the sampling points in the Sleeper vein (sample from the 4040 Bench in the Sleeper mine)

The high-grade ores and banded nature of the ores (formed by deposition of progressive layers along vein walls over time) allowed for a precise determination of mineral relationships. In particular, ore and gangue minerals chosen for isotopic analysis came from bands that contained abundant Au-Ag minerals. This was accomplished by microdrilling of individual minerals or by dissolution and disaggregation of bulk samples by cold or hot hydrogen fluoride (HF). In the latter procedure, minerals were hand-picked using a binocular microscope to separate them. Minerals for analysis were then dissolved for Cu and Pb isotopic analyses with a

multicollector inductively coupled plasma mass spectrometry (ICP-MS) or by standard combustion techniques for S isotopes. Because of the abundance of chalcopyrite in close association with Au-Ag minerals in these bonanza ores, it was targeted for our S isotope analyses and also much of the Cu isotope analyses. However, the ore mineral electrum and naumannite-agularite typically contain enough Cu and Pb (>10 ppm) to allow measurement of their Cu and Pb isotopic ratios. Similarly, physically separated gangue minerals (quartz, opal, adularia, or quartz+adularia) also contain enough Pb for isotopic analysis.

Table 2 Sulfur and copper isotope data for epithermal ores from the northern Great Basin (USA) and Japan

Sample location	Sample number	Phase measured	$\delta^{34}\text{S}$ (‰)	$\delta^{65}\text{Cu}$ (‰)
Buckskin National	Buck-1	nm	-0.6	-0.087
Buckskin National	Buck-2	cpy, nm	-5.3	-0.351
Buckskin National	Buck-3a	el, nm		0.639
Buckskin National	Buck-3b	nm		0.560
Buckskin National	Buck-4	nm, cpy		-0.501
Buckskin National	Buck-5	cpy	-5.7	0.860
Buckskin National	Buckkin-1	nm		0.830
Buckskin National	Buckkin-2	cpy		-0.150
National	NL-2	el		-1.166
Sleeper	SL-2	el		-1.574
Sleeper	Sleeper	el		0.120
Jumbo	J-1	el		-1.574
Seven Troughs	7T-1	nm		-0.383
Midas	Mid-1	cpy	3.5	1.131
Midas	Mid-1	cpy	-1.6	0.630
Midas	Mid-2	El	3.4	1.516
Midas	Mid-3	nm		-0.823
Midas	Mid-3	cpy		1.465
Midas	Mid-3	el		1.287
Midas	Mid-4c	nm		-0.854
Midas	Mid-5a	el, nm		3.254
Midas	Mid-5a	nm, el		-0.276
Midas	Mid-5b	cpy		-0.363
Midas	Mid-5b	nm	2.7	1.114
Midas	Mid-5c	el		3.211
Midas	Midas	nm		1.620
Ivanhoe/Hollister	IV-1	el, nm, cpy		0.693
Ivanhoe/Hollister	IV-2	el, nm		0.724
Ivanhoe/Hollister	Ivanhoe	nm		0.460
Koryu	Ku-1	cpy		0.145
Koryu	Ku-2	cpy		1.317
Koryu	Ku-4	cpy		0.605
Hishikari	HK-1	cpy, nm		-0.588
War Eagle Mtn.	Poorman	nm		-1.151
DeLamar Mtn.	DEL-1	nm		0.851
DeLamar Mtn.	DEL-2	nm		-1.301
DeLamar Mtn.	DEL-3	el		-2.704
Trade Dollar Mine	TD-1	cpy	-0.4	0.422
Trade Dollar Mine	TD-1	cpy	-2.3	0.651
Trade Dollar Mine	TD-1	cpy	-0.1	-0.145
Trade Dollar Mine	TD-2	cpy	-7.0	
Trade Dollar Mine	TDollar	cpy		0.090
Dewey Mine	Dew-1	cpy	0.0	
Dewey Mine	Dew-1	cpy	-2.1	
Dewey Mine	Dew-2	cpy	-0.1	
Idaho Tunnel	IT-1	cpy	0.3	
Idaho Tunnel	IT-1	cpy	-3.2	
Idaho Tunnel	IT-2	cpy	0.3	

el electrum, *cpy* chalcopyrite, *nm* naumannite,

Cu isotope measurements on chalcopyrite were conducted using similar techniques as described in Mathur et al. (2010). Electrum and naumannite were dissolved in Teflon beakers with 8 ml of ultrapure aqua regia at 140 °C for 24 h or until complete dissolution occurred. Concentrations of copper were measured from these solutions on an ICP-MS to determine the amount of solution to dry for purification by ion exchange chromatography. Concentrations ranged from 12 to 220 ppm Cu in electrum and naumannite, and a volume that contained 1 µg of copper was dried and used for ion exchange chromatography. The exchange chromatography, mass spectrometry preparation, and measurement methods are identical to Mathur et al. (2010).

Chalcopyrite samples were used to measure S isotopic ratios. Samples were weighed, mixed with V₂O₅, CuO, and quartz, and then milled. Samples were then placed in a combustion tube, were thoroughly dried, and then heated in a furnace at 1050 °C. H₂O and CO₂ were removed from SO₂, which was then analyzed for S isotope ratios in a mass spectrometer at the University of Georgia.

The fine-grained nature of electrum from the Sleeper deposit made it impossible to physically separate enough of it for Pb isotope analyses. Thin (2–3 mm) slices were cut perpendicular to banding, and ore and gangue minerals were subsequently separated chemically. Sample cleaning and Pb separation was done under clean lab environment at the Department of Geological Sciences at the University of Florida. The separated vein pieces were cleaned by sonication with Optima-grade acetone multiple times then rinsed with 4× H₂O. After the acetone cleaning, each piece was transferred to a precleaned Teflon vial and was cleaned overnight with warm Optima-grade 3.5 N HNO₃. The nitric acid was discarded, and the vein piece was again rinsed multiple times with 4× H₂O. Concentrated Optima-grade HF was added to the clean vein sample and left overnight on the hot plate with the Teflon vial closed to dissolve the silicate fraction. The following day, the resultant HF solution was transferred to a clean Teflon vial. The remaining electrum looked clean and free of any silicates, but as a precaution, was subjected to another leaching with clean Optima-grade HF. The second batch of HF was added to the first, and all of the HF was evaporated to dryness. This HF residue constitutes the gangue fraction that was subsequently processed for Pb isotope analysis. In brief, Pb from the silicate (HF) fraction was purified on Dowex 1×-8 resin in traditional 1 N HBr medium; details are provided in Kamenov et al. (2013). The separated clean electrum after the double HF attack was rinsed multiple times with 4× H₂O, then leached overnight in warm 3.5 N HNO₃, then rinsed again with 4× H₂O and dissolved with aqua regia. Pb was separated from the electrum also following protocol described in Kamenov et al. (2013). In brief, the resultant aqua regia solution was evaporated to dryness, and the electrum residue was dissolved in 2 ml 6 N HCl. The 6 N HCl solution was loaded on columns

packed with Dowex 1×8 resin and the elutant was collected in a clean Teflon vial. The gold-free solution was then evaporated to dryness, and Pb was further purified with 1 N HBr. Pb isotopic compositions for all samples were determined on an Nu-Plasma MC-ICP-MS with Tl normalization following a method described in Kamenov et al. (2004). Long-term analysis of the NBS 981 Pb isotope standard yielded the following average values: ²⁰⁶Pb/²⁰⁴Pb=16.937 (±0.004, 2σ), ²⁰⁷Pb/²⁰⁴Pb=15.490 (±0.003, 2σ), and ²⁰⁸Pb/²⁰⁴Pb=36.695 (±0.009, 2σ).

Results

The use of copper isotopes in ore deposit research is a new and evolving field (Li et al. 2010; Mathur et al. 2010; Wall et al. 2011; Asadi et al. 2015). Cu isotopic ratios were measured on the three principal (and coexisting) phases in these ores (e.g., Fig. 2a): electrum, naumannite, and chalcopyrite. Results indicate δ⁶⁵Cu values range between approximately −2.5 and +3.5‰, with most values falling between −1 and +1‰ (Fig. 3). The latter range is very similar to δ⁶⁵Cu values for porphyry copper deposits which are generally interpreted to have formed from magmatic fluids, metals, and sulfur (Li et al. 2010; Asadi et al. 2015).

Copper isotope values also overlap with δ⁶⁵Cu values of “mantle” rocks and metallic meteorites (Bishop et al. 2012; Fig. 3). Further, all three of these phases yield similar results from the same samples indicating a certain degree of isotopic equilibrium between ore minerals and a similarity of δ⁶⁵Cu values between principal districts studied here (Fig. 4). Given our current limited understanding of Cu isotope fractionation

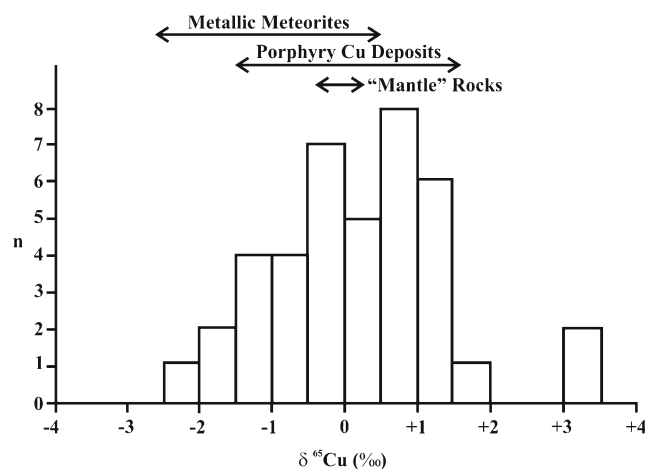
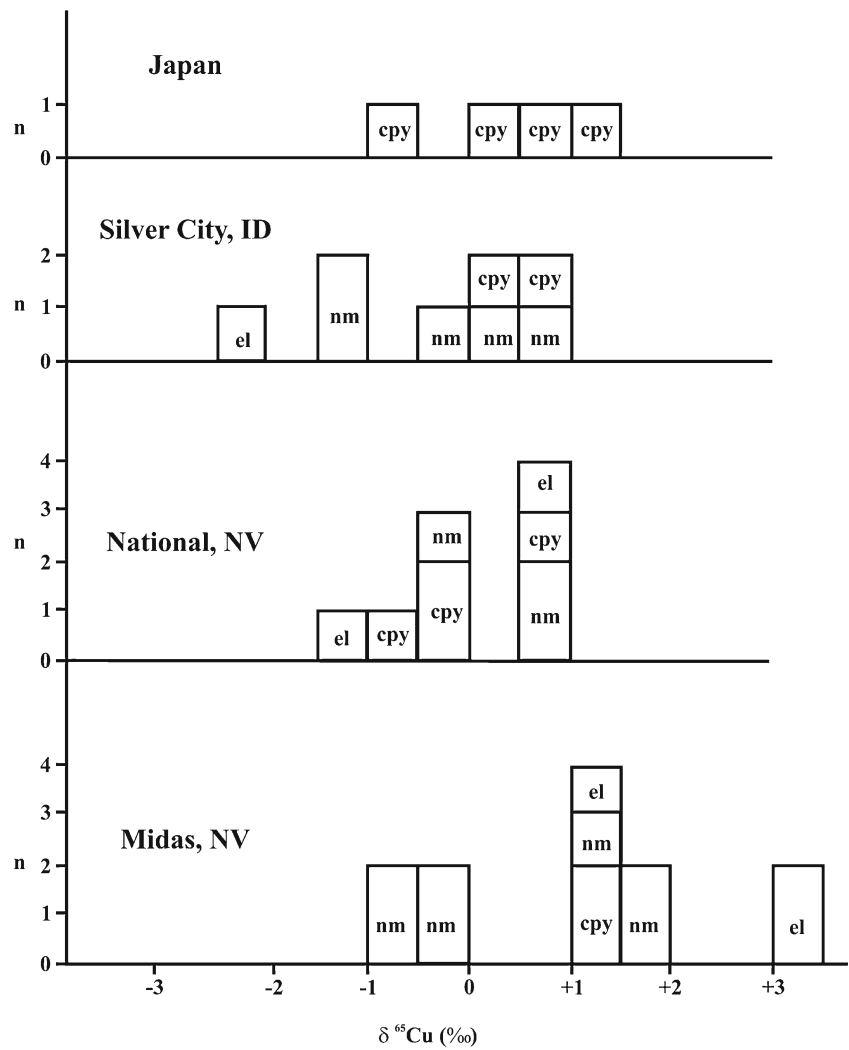


Fig. 3 Histogram showing δ⁶⁵Cu in ‰ from western USA (northern Great Basin) and Japanese epithermal ores. Data for “mantle rocks” and iron meteorites from Bishop et al. (2012) and for porphyry deposits from Li et al. (2010) and Asadi et al. (2015). Zero per thousand (0‰) is the value assigned to the NIST copper standard

Fig. 4 Histogram subsets of $\delta^{65}\text{Cu}$ data for specific districts, showing mineral phases that Cu isotope data were measured on. Mineral abbreviations are the same as in Fig. 2



during the formation of a number of different ore deposit types, we do not have sufficient data at this point to fully characterize all types of copper or copper-bearing deposits. However, data presented here show that Cu isotope signature of Cu-bearing epithermal minerals is surprisingly similar to those from the center of porphyry copper (e.g., formed at much higher temperature). All $\delta^{34}\text{S}$ values measured in this study were only from NGB epithermal ores, and all values determined were from chalcopyrite, as it is by far the most abundant sulfide mineral in the Au-Ag-rich bands in the ores. At epithermal temperatures (~150–300 °C), $\delta^{34}\text{S}$ of chalcopyrite is essentially equal to the $\delta^{34}\text{S}$ value of aqueous sulfide in the ore-forming fluids (Seal 2006). Results (Fig. 5) show $\delta^{34}\text{S}$ ranging from ~-7 to +4‰ with about half of the values falling between -1 and +1‰, values that are generally interpreted to be indicative of a principal magmatic source of sulfur (Seal 2006). Due to extensive published sulfur isotope data from the two Japanese deposits and the more reconnaissance nature of our copper isotope investigations there, we did not analyze $\delta^{34}\text{S}$ values for those ores. However, published data from

the high-grade “ginguro” bands from Hishikari (-1 to +2‰; Shikazono 1999) and Koryu (-3.9 to +2.7‰, mean ~0‰; Shimizu et al. 1998) are similar to NGB epithermal ores (John et al. 2003; Fig. 5), as are recent $\delta^{34}\text{S}$ data from

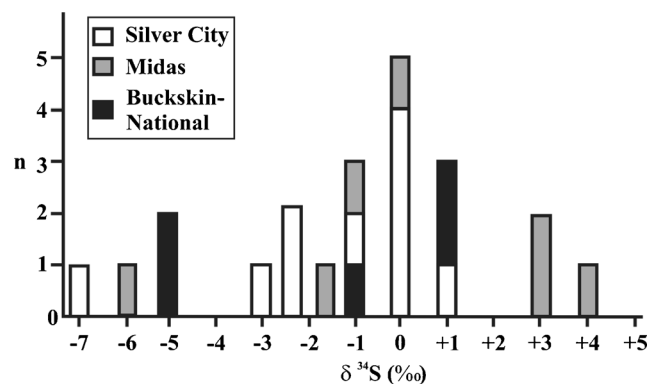


Fig. 5 Histogram showing $\delta^{34}\text{S}$ in per thousand from the northern Great Basin (USA) epithermal ores; all data are from chalcopyrite

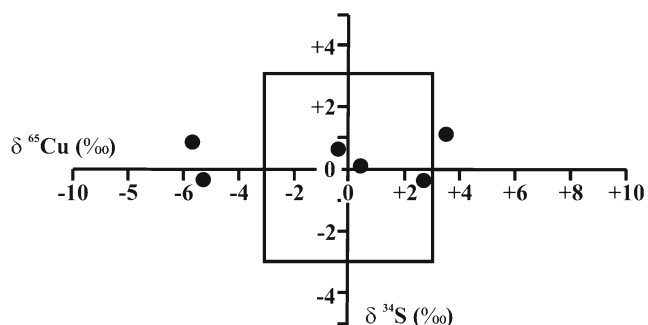


Fig. 6 Plot of $\delta^{34}\text{S}$ versus $\delta^{65}\text{Cu}$ data for six chalcopyrite samples from epithermal deposits in the northern Great Basin for which both parameters were measured. The highlighted box is the typical range of $\delta^{34}\text{S}$ and $\delta^{65}\text{Cu}$ values for porphyry copper deposits

epithermal ores in New Zealand (Christie et al. 2007), Indonesia (Yuningsih et al. 2011), and Kamchatka (Takahashi et al. 2012). Plotting both Cu and S isotope values measured on the same chalcopyrite grains from the NGB epithermal ores also shows a range of values similar to “magmatic” porphyry copper ores (Fig. 6).

In the process of conducting our earlier Pb isotopic investigations (Kamenov et al. 2007), we observed data that suggested that the Pb isotopic composition of electrum was different from adularia codeposited with the gold. In particular, here, we evaluated that finding at the Sleeper deposit (Fig. 7). Pb isotope data show disequilibrium between the gold ore and the silicate fraction that cannot be explained with in situ U and Th decay. The observed trend in Pb-Pb isotope space suggests distinct sources for gold and gangue minerals in the epithermal hydrothermal system (Fig. 8). The silicate minerals show elevated $^{207}\text{Pb}/^{204}\text{Pb}$ indicating that the elements composing the gangue are most likely leached from local sedimentary or metamorphic rocks. In contrast, the gold ore shows lower $^{207}\text{Pb}/^{204}\text{Pb}$ indicating derivation from a likely deeper, mafic magmatic source, supporting the S and Cu isotope data. The observed Pb isotope disequilibrium between gangue and electrum occurs at the millimeter to centimeter scale within the epithermal vein.

Fig. 7 Photograph of banded bonanza ore from the Sleeper deposit, exhibiting at least seven different electrum-rich bands, which was used for the Pb isotope investigation described in the text; sample numbers correspond to those listed in Table 1

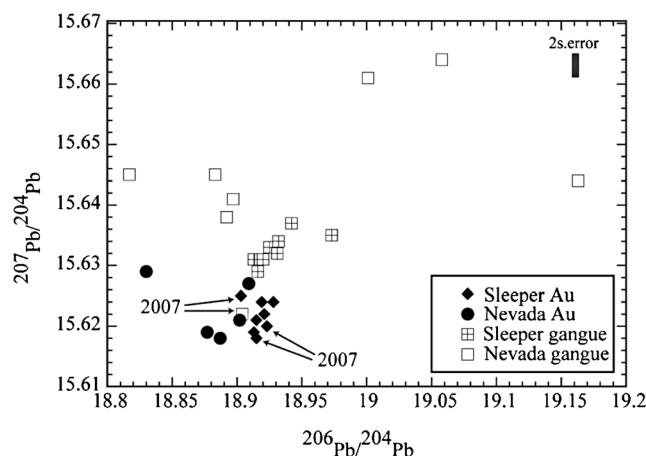
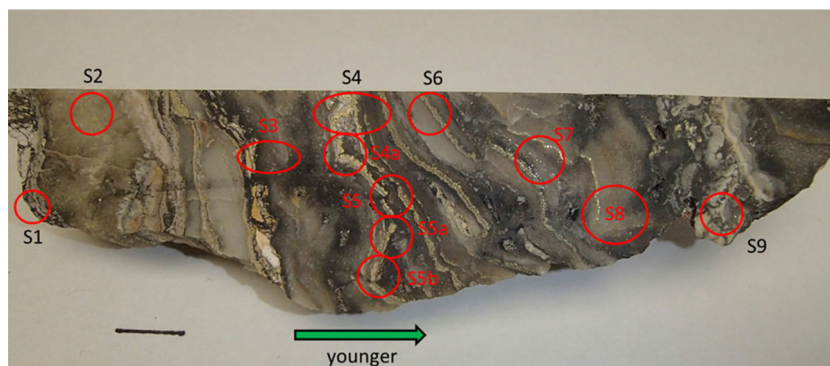


Fig. 8 Plot of lead isotope data for Sleeper deposit (NV) electrum and gangue from this work compared to northern Nevada epithermal ores and gangue data from Kamenov et al. (2007). “Nevada Au” includes data from Jumbo, National, Seven Troughs and Sleeper and “Nevada gangue” includes data from Jumbo, National, Sleeper, New Alma, and Sandman. Arrows point to the three Sleeper electrum samples and the one Sleeper gangue sample reported in Kamenov et al. (2007). Bar in the upper right corner represents the two standard errors of the Pb isotope measurements

Discussion

Recent research has shown that the subduction process can prepare the lithospheric mantle for later “fertile” magma partial melts to form in the mantle, which then can rise through the crust and trigger ore formation (Richards 2009; Saunders and Brueske 2012). Thus, a postsubduction mantle plume (western USA) or rift-triggered partial melting (Japan) can apparently trigger partial melting of this “fertilized” lithospheric mantle and can lead to volcanism and related epithermal ore formation.

The Japanese and NGB bonanza epithermal ores are enriched in Se, thus Lindgren (1933) would have classified the deposits considered here as “gold-selenide” epithermal ores. Saunders (2012) noted that these ores are also enriched in copper due to their abundance of chalcopyrite in highest-grade ores, and interpreted the Cu enrichment (along with

gold) to result from a mafic magmatic source. In fact, at Hishikari, gold shows a stronger statistical correlation with copper than either silver or selenium (Nagayama 1993). The present study indicates a predominant magmatic origin for Cu and S. This is consistent with previous Pb isotope data on electrum from NGB mid-Miocene epithermal ores that indicated a primitive (mafic) magmatic origin for gold (Kamenov et al. 2007); Re-Os isotope data from these ores suggest a similar origin (Saunders et al. 2014). Further, the Pb isotopic disequilibrium between ore and gangue minerals in NGB epithermal ores indicates distinct sources for the two materials. O and H isotopes indicate a predominant meteoric water source for ore-forming solutions in the Japanese deposits of Hishikari (Hayashi et al. 2000; Faure et al. 2002) and Koryu (Shimizu et al. 1998), as well as the NGB ores (John et al. 2003; Saunders et al. 2008), an interpretation which is generally consistent with fluid inclusion microthermometric data (Izawa et al. 1990; Shimizu et al. 1998; John et al. 2003). As discussed above, textures in NGB and Japanese bonanza epithermal ores show evidence of silica and metallic nanoparticle physical transport and aggregation (Saunders 1990, 1994, 2012). Thus, any model for the genesis of these ores must account for (1) bonanza ore textures that demonstrate nanoparticle transport and aggregation; (2) isotopic evidence that metals and sulfur had a predominant magmatic source; (3) the Pb isotopic disequilibrium for ore and gangue minerals; and (4) that the ore-forming solutions were predominantly heated meteoric waters.

The idea that gold (and silver) nanoparticles can form in epithermal ore-forming systems perhaps dates back about a century, stemming from Lindgren's research on the National deposit, Nevada (Lindgren 1915, 1933). More recently, evidence from ore textures in bonanza epithermal ores in western USA (Saunders 1990, 1994, 2012, and references therein) and elsewhere (Marinova et al. 2014) have provided additional support to the concept. Further, gold nanoparticles have been identified in the Champagne Pool, New Zealand (Pope et al. 2005), and metallic-sulfide nanoparticles also occur entrained in fluids discharging from seafloor hydrothermal vents (Yucel et al. 2011). Gold nanoparticles have been observed depositing from volcanic vapors (Meeker et al. 1991; Fulignati and Sbrana 1998; Taran et al. 2000; Yudovskaya et al. 2006); Hough et al. (2008) describe other environments where gold nanoparticles occur. Textural data from western USA bonanza ores show that aggregation of nanoparticles of Au-Ag alloy, Ag-Se-S phases, and chalcopyrite is an important ore-forming process (Saunders 2012).

There is difficulty in reconciling data that show epithermal ore-forming solutions were predominantly shallow meteoric water with our isotopic data indicating that metals and sulfur have a magmatic origin. Saunders et al. (2008) attempted to explain this disparity for NGB ores by invoking a two-hydrothermal solution model: (1) a shallow geothermal

system driven by the magmatic heat source at depth which leaches major elements from surrounding country rocks required to make the gangue minerals in veins and (2) episodic incursions of magmatic components into the shallower geothermal system, which causes the banded nature of ore and repeated deposition of ore minerals over time. That model was largely based on geologic and hydrothermal conditions at present-day Yellowstone National Park, USA (Lowenstern and Hurwitz 2008). At Yellowstone, a shallow rhyolitic magma chamber is interpreted to be the heat source for the world's largest geothermal system, but deeper basaltic magmas apparently contribute magmatic volatiles (including sulfur) episodically to the shallow geothermal system (Lowenstern and Hurwitz 2008). So, if magma bodies at depth are the source of metals, metalloids, and sulfur (and selenium) that are incorporated into the shallow epithermal ores, how does this occur? One hypothesis is that volatile metals and sulfur are transported to the epithermal environment (and mix with the shallow geothermal waters) in low-density magmatic "vapors" that contribute magma-sourced metals but little water (Hedenquist and Lowenstern 1994; Heinrich et al. 2004; Williams-Jones and Heinrich 2005). Would nucleation of Au-Ag-Cu minerals directly in the shallow, low-temperature, epithermal setting preserve magmatic isotopic signatures for those minerals? It seems more likely that Au-Ag-Cu phases nucleated as nanoparticles at depth and were physically transported to the epithermal environment. In the process, higher-temperature magmatic Cu, Pb, and S isotopic signatures were preserved, and ores formed by particle aggregation along vein walls. Saunders (1994) proposed that Au-Ag nanoparticles formed directly in the epithermal environment in response to boiling of ore-forming solutions. Isotopic data presented by Kamenov et al. (2007) and in this study make that interpretation less likely and support a deeper origin for the nanoparticles.

Conclusions

The first Cu isotope data from definitive ore-stage Au-Ag minerals in epithermal ores (and Cu and S isotopes on associated chalcopyrite) indicate a deeper magmatic source of metal(oids) and sulfur in these shallow LS bonanza ores. It is likely that this is not just the case for bonanza ores, but may also apply to other epithermal ores or even to other hydrothermal gold deposits. The bonanza ores provide the context for interpreting the timing of ore- and gangue-mineral deposition, show that ore mineral precipitation occurred episodically over time, and provide abundant (and large) minerals for isotopic analysis. Our new Pb isotope data, building on the previous work of Kamenov et al. (2007), show that ore and closely associated gangue minerals have a different source of Pb.

This provides further support to the model of Saunders et al. (2008) that a deeper magmatic source of metal(oids) and sulfur is mixed with a shallow geothermal fluid that is leaching major elements (e.g., K, Al, Na, and Si) from the surrounding shallow host rocks to make the principal vein gangue minerals. This conclusion has implications for fluid inclusion and isotope studies that have focused on using the gangue minerals for analysis, if those minerals do indeed have principally different sources.

The isotopic data presented here are consistent with episodic introduction of metal(oids) and sulfur from a deeper magmatic source into the shallow epithermal-geothermal setting. Present-day geothermal systems are analogs of epithermal systems, but the implications from the data presented here are that (1) it is highly unlikely that geothermal systems consisting of only heated meteoric water form epithermal ore deposits, and (2) a necessary component for making an epithermal ore deposit is the presence of magma with the right composition below the epithermal system, tectonic history, and structural setting in the crust. The LS epithermal ores of the western USA (NGB) and Japan formed in tectonic settings that allowed for partial melting of a fertile lithospheric mantle, generation of metal S-rich basaltic partial melts, which rose to shallow levels in the crust and triggered ore formation (and often bimodal volcanism). Thus, the tectonic setting and the composition of the mafic magmas are perhaps what should be evaluated and focused on for exploration for new epithermal deposits.

From the exploration standpoint, it is irrelevant if the deeper magmas episodically introduced ore constituents as “vapors” or physically transported nanoparticles that probably formed from cooling and condensing of such vapors along (or both processes in concert) with the upward rise of the magmatic fluids. Nanoparticle aggregation likely provided an efficient mechanism to facilitate the characteristic high grades of these ores, but not the total amount of metal endowments present in the deposits. In the epithermal setting, cooling and boiling of the epithermal solutions can lead to further metal and silica deposition at the same time as existing silica and nanoparticles are aggregating along vein walls. Thus, in summary, a minor contribution of magmatic fluids mixing with the shallow meteoric water-dominated geothermal system would not appreciably change the O and H isotopic composition of the ore-forming system, but that small fraction of magmatic fluid contributes essentially all the metal(oid)s and sulfur to the shallow ore-forming solutions. Implications of these results profoundly affect exploration strategies for these ores, which previously often focused on exploring for fossil geothermal systems. Instead, exploration should focus on the geotectonic settings that produce the right type of magmas capable of releasing metal-rich fluids necessary to form epithermal ores and deeper deposits as well.

Acknowledgments Funding for this research was provided by grants to JAS (EAR- 0838208; EAR-1247857) and MEB (EAR-0838139) from the NSF. Erin Summerlin and Mike Mason conducted the S isotope work at the University of Georgia, with the assistance of Doug Crowe at UGA. We also thank Michelle Burke of Miami University for the SEM of a fractal dendrite from the Sleeper deposit.

References

- Asadi S, Mathur M, Moore F, Zarasvandi A (2015) Copper isotope fractionation in the Meiduk porphyry copper deposit, Northwest of Kerman Cenozoic magmatic arc, Iran. *Terra Nova*, 27:36–41
- Bishop MC, Moynier F, Weinstein C, Fraboulet J-G, Wang K, Foriel J (2012) The Cu isotopic composition of iron meteorites. *Meteor Plan Sci* 47:268–276
- Christie AB, Simpson MP, Brathwaite RL, Mauk JL, Simmons SF (2007) Epithermal Au-Ag and related deposits of the Hauraki Goldfield, Coromandel Volcanic Zone, New Zealand. *Econ Geol* 102:785–816
- Faure K, Matsuhsa Y, Metsugi H, Mizota C (2002) The Hishikari Au-Ag epithermal deposit, Japan: oxygen and hydrogen isotope evidence in determining the source of paleohydrothermal fluids. *Econ Geol* 97: 481–498
- Foley NK, Ayuso RA (2012) Gold deposits of the Carolina Slate Belt, southeastern United States—age and origin of the major gold producers. USGS Op-File Rept 2012-1179., p 30
- Fulignati P, Sbrana A (1998) Presence of native gold and tellurium in the active high-sulfidation hydrothermal system of the La Fossa volcano (Vulcano, Italy). *J Volc Geotherm Resc* 86:187–198
- Hayashi K, Maruyama T, Satoh H (2000) Submillimeter scale variation of oxygen isotopes of vein quartz at the Hishikari Deposit, Japan. *Resource Geol* 50:141–150
- Hedenquist JW, Lowenstern JB (1994) The role of magmas in the formation of hydrothermal ore deposits. *Nature* 370:519–527
- Heinrich CA, Driesner T, Stefansson A, Seward TM (2004) Magmatic vapor contraction and the transport of gold from the porphyry environment to epithermal ore deposits. *Geology* 32:761–764
- Hough RM, Noble RRP, Hitchen GJ et al (2008) Naturally occurring gold nanoparticles and nanoplates. *Geology* 6:71–74
- Izawa E, Urashima Y, Ibaraki K et al (1990) The Hishikari gold deposit: high grade epithermal veins in quaternary volcanics of southern Kyushu, Japan. *J Geochem Explor* 36:1–56
- John DA, Hofstra AH, Fleck RF, Brummer JE, Saderholm EC (2003) Geologic setting and genesis of the Mule Canyon low-sulfidation epithermal gold-silver deposit, North-Central Nevada. *Econ Geol* 98:425–463
- Kamenov GD, Mueller P, Perfit M (2004) Optimization of mixed Pb-Tl solutions for high precision isotopic analyses by MC-ICP-MS. *J Anal A Spectrom* 19:1262–1267
- Kamenov GD, Saunders JA, Hames WE, Unger D (2007) Mafic magmas as sources for gold in middle-Miocene epithermal deposits of northern Great Basin, USA: evidence from Pb isotopic compositions of native gold. *Econ Geol* 102:1191–1195
- Kamenov GD, Melchiorre EB, Ricker FN, DeWitt E (2013) Insights from Pb isotopes for native gold formation during hypogenic and hypergenic processes at Rich Hill, Arizona. *Econ Geol* 108:1577–1589
- Li W, Jackson SE, Pearson NJ, Grahma S (2010) Copper isotopic zonation in the Northparkes porphyry Cu–Au deposit, SE Australia. *Geochim Cosmochim Acta* 74:4078–4096
- Lindgren W (1915) Geology and mineral deposits of the national mining district, Nevada. US Geol Surv Bull 601:58
- Lindgren W (1933) Mineral deposits, 4th edn. McGraw Hill, New York

- Lowenstern JB, Hurwitz S (2008) Monitoring a supervolcano in repose: heat and volatile flux at the Yellowstone Caldera. *Elements* 4:35–40
- Marinova I, Ganey V, Titorenkova R (2014) Colloidal origin of colloform-banded textures in the Paleogene low-sulfidation Khan Krum gold deposit, SE Bulgaria. *Mineral Deposita* 49:49–74
- Mathur R, Dendas M, Titley S, Phillips A (2010) Patterns in the copper isotope composition of minerals in porphyry copper deposits in southwestern United States. *Econ Geol* 105:1457–1467
- Matsuhisa Y, Aoki M (1994) Temperature and oxygen isotope variations during formation of the Hishikari epithermal gold-silver veins, southern Kyushu, Japan. *Econ Geol* 89:1608–1613
- Meeker KA, Chuan RL, Kyle PR, Palais JM (1991) Emission of elemental gold particles from Mount Erebus, Ross Island, Antarctica. *Geoph Res Lett* 18:1405–1408
- Nagayama T (1993) Precipitation sequence of veins at the Hishikari deposits, Kyushu, Japan. *Resource Geol Spec Issue* 14:13–28 (**Japan**)
- O'Neil JR, Silberman ML, Fabbri BP, Chesterman CW (1973) Stable isotope and chemical relations during mineralization in the Bodie Mining District, Mono County, California. *Econ Geol* 68:765–784
- Pope JG, Brown KL, McConchie DM (2005) Gold concentrations in springs at Waioatapu, New Zealand: implications for precious metal deposition in geothermal systems. *Econ Geol* 100:677–687
- Richards JP (2009) Post-subduction porphyry Cu-Au and epithermal Au deposits: products of remelting of subduction-modified lithosphere. *Geology* 37:247–250
- Saunders JA (1990) Colloidal transport of gold and silica in epithermal precious metal systems: evidence from the Sleeper deposit, Humboldt County, Nevada. *Geology* 18:757–760
- Saunders JA (1994) Silica and gold textures at the Sleeper deposit, Humboldt County, Nevada: evidence for colloids and implications for ore-forming processes. *Econ Geol* 89:628–638
- Saunders JA (2012) Textural evidence of episodic introduction of metallic nanoparticles into bonanza epithermal ores. *Minerals* 2:228–243
- Saunders JA, Schoenly PA (1995) Boiling, colloid nucleation and aggregation, and the genesis of bonanza gold mineralization, Sleeper deposit, Nevada. *Mineral Deposita* 30:199–211
- Saunders JA, Brueseke ME (2012) Volatility of metal(loids) and the geochemistry of epithermal Au-Ag ores in western USA. *Econ Geol* 107:165–172
- Saunders JA, Unger DL, Kamenov GD, Fayek M, Hames WE, Utterback WC (2008) Genesis of Middle Miocene Yellowstone-hotspot-related bonanza epithermal Au-Ag deposits, Northern Great Basin Region, USA. *Mineral Deposita* 43:715–734
- Saunders JA, Hofstra AH, Goldfarb RJ, Reed MH (2014) Geochemistry of hydrothermal gold deposits. In: Holland HD, Turekian KK (eds) *Treatise on Geochemistry*, vol 13, 2nd edn. Elsevier, Oxford, pp 383–424
- Seal RR II (2006) Sulfur isotope geochemistry of sulfide minerals. *Rev Min Geochem* 61:633–677
- Shikazono N (1999) Sulfur isotope composition and origin of sulfide sulfur in epithermal Au-Ag vein-type deposits in Japan. *Resource Geol Spec Issue* 20:39–45
- Shimizu T, Matsueda H, Ishiyama D, Matsubaya O (1998) Genesis of epithermal Au-Ag mineralization of the Koryu Mine, Hokkaido, Japan. *Econ Geol* 93:303–325
- Sillitoe RH, Hedenquist JW (2003) Linkages between volcano tectonic settings, ore-fluid compositions, and epithermal precious metal deposits. *Soc Econ Geol Spec Pub* 10:315–343
- Simmons SF, White NC, John DA (2005) Geological characteristics of epithermal precious and base metal deposits. 100th Anniv Vol *Econ Geol* 485-522
- Takahashi R, Matsueda H, Okrugin VM (2012) Ore-forming ages and sulfur isotope study of hydrothermal deposits in Kamchatka, Russia. *Res Geol* 63:210–223
- Taran YA, Bernard A, Gavilanes JC, Africano F (2000) Native gold in mineral precipitates from high-temperature volcanic gases of Colima volcano, Mexico. *Appl Geochem* 15:337–346
- Wall AJ, Mathur R, Post JE, Hearney PJ (2011) Cu isotope fractionation during bornite dissolution: an in situ X-ray diffraction analysis. *Ore Geol Rev* 42:62–70
- Williams-Jones AE, Heinrich CA (2005) Vapor transport of metals and the formation of magmatic-hydrothermal ore deposits. *Econ Geol* 100:1287–1312
- Yucel M, Gartman A, Chan CS, Luther GW III (2011) Hydrothermal vents as a kinetically stable source of iron-sulphide-bearing nanoparticles to the ocean. *Nature Geosci* 4:367–371
- Yudovskaya MA, Distler VV, Chaplygin IV et al (2006) Gaseous transport and deposition of gold in magmatic fluid: evidence from the active Kudryavy volcano, Kurile Islands. *Miner Deposita* 40:828–848
- Yuningsih ET, Matsueda H, Rosana MF, Aryani SC (2011) Physicochemical conditions of the Se- and Te-types of epithermal Au-Ag deposits of western Java, Indonesia. *Geol Assoc Canada/Mineral Assoc Canada, Abstracts* 34:237–238